Available online at www.sciencedirect.com
ScienceDirect
Journal of Power Sources 160 (2006) 1–9
JOURNAL OF POWER SOURCES
www.elsevier.com/locate/jpowsour

# Characteristics of droplet and film water motion in the flow channels of polymer electrolyte membrane fuel cells

Zhigang Zhan [a,b], Jinsheng Xiao [a,c,*], Mu Pan [a], Runzhang Yuan [a]

[a] State Key Laboratory of Advanced Technology for Materials Synthesis and Processing, Wuhan University of Technology, Hubei 430070, China
[b] School of Energy and Power Engineering, Wuhan University of Technology, Hubei 430070, China
[c] School of Automotive Engineering, Wuhan University of Technology, Hubei 430070, China

Received 3 October 2005; received in revised form 25 November 2005; accepted 21 December 2005
Available online 9 February 2006

**Abstract**

Characteristics of droplet and film water motion in the flow channels of polymer electrolyte membrane fuel cells (PEMFCs) have important influence to cell performance, but the moving mechanism is not clear. Considering for the first time the hydrophilicity of graphite plate (GP) and the hydrophobicity of the gas diffusion layer (GDL), which form the walls of the gas channel, using the volume-of-fluid (VOF) model of FLUENT software, the motion of liquid water under different Weber numbers (or different gas velocities) was simulated in a straight channel and a serpentine channel. The results show that the hydrophilicity of GP and the hydrophobicity of GDL play an important role in the liquid water motion; the more hydrophobic the surfaces of the channel are, the more easily the water is to be discharged. Liquid water can be attracted from GDL onto the hydrophilic walls of the GP, which is beneficial to the diffusion of oxygen from the gas channel to the catalyst layer. When Weber number is larger than 4.4 (gas velocity is lower than 4 m $s^{-1}$), effects of surface tension and wall surface adhesion on the motion of liquid water in the gas channel are very obvious; when Weber number is less than 4.4 (gas velocity is higher than 4 m $s^{-1}$), inertia force plays the main role in the motion of liquid water in the gas channel. Liquid water is easier to be discharged under high velocity than under lower velocity, and in the straight channel than in the serpentine channel.


*Keywords:* Polymer electrolyte membrane fuel cell; Hydrophilic; Hydrophobic; Surface tension; Wall surface adhesion

## 1. Introduction

The application prospect of polymer electrolyte membrane fuel cell (PEMFC) is promising, but at present its cost is still too high and its performance is unstable, the basic reason is that its internal mechanism has not been fully understood, and the function, production, phase change and transportation of water in fuel cells is one of many problems, which people haven't known well and are studying widely. A lot of papers are about these areas, but relatively people pay more attention to the function and transportation mechanism of water in proton exchange membrane [1,2], catalyst layer [3] and gas diffusion layer (GDL) [4,5]; characteristics of liquid water motion in the flow channels are less studied. For the papers of this respect, Geiger et al. [6] and Satija et al. [7] studied the neutron radial method to investigate the gas/liquid two-phase flow in the PEMFC flow channels, but some technologic problems to be solved. Through a transparent fuel cell, Tuber et al. observed directly the phenomena that the liquid water seeped out from the diffusion layer to the gas channel and formed a small droplet, then the droplet grew up and blocked the channel, they also measured the variation of fuel cell performance with the flooding state in the gas channels, and probed into the effects of different air flux, different operating temperature, different air humidity and the hydrophobicity of the GDL on the cell performance [8]. A similar work was done by Yang et al. [9], but the influence of the surface adhesion to the size to which the droplets could grow in the gas channels, liquid film formation on hydrophilic walls were further observed and analyzed. As for modeling, water in gas channels is often supposed as ideal gas, i.e. no liquid water over there at all, or water droplets present, but the size is so small that they can be considered as gas state [10–13]. Peng et al. mod-

* Corresponding author at: 122 Luoshi Road, State Key Laboratory of Advanced Technology for Materials Synthesis and Processing, Wuhan University of Technology, Hubei 430070, China. Tel.: +86 27 131 1439x5196; fax: +86 27 8785 9223.
*E-mail address:* jsxiao@mail.whut.edu.cn (J. Xiao).

0378-7753/$ – see front matter © 2006 Elsevier B.V. All rights reserved.
doi:10.1016/j.jpowsour.2005.12.081

**Nomenclature**

| | |
|---|---|
| $Ca$ | Capillary number |
| $d$ | hydraulic diameter (m) |
| $F$ | momentum source item (N m$^{-3}$) |
| $g$ | acceleration of gravity (m s$^{-2}$) |
| $k$ | curvature of the interface of two phases |
| $Re$ | Reynolds number |
| $\vec{u}$ | velocity vector (m s$^{-1}$) |
| $We$ | Weber number |

*Greek letters*

| | |
|---|---|
| $\alpha$ | phase fraction |
| $\mu$ | dynamic viscosity (Pa s) |
| $\nu$ | kinematic viscosity (m$^2$ s$^{-1}$) |
| $\rho$ | density (kg m$^{-3}$) |
| $\sigma$ | surface tension (N m$^{-1}$) |

*Subscripts*

| | |
|---|---|
| g | gas |
| l | liquid |
| $q$ | the $q$th phase |

eled firstly the liquid water motion in a serpentine channel with volume-of-fluid (VOF) model of FLUENT software [14], the behaviors of different number and positions of water droplets, and of different thickness of water films, were investigated. Jiao et al. presented a numerical investigation of air/water flow in parallel serpentine channels on cathode side of a PEFC stack by use of FLUENT. Different air/water flow behaviors inside the serpentine flow channels were discussed, and found there were significant variations of water distribution and pressure drop in different cells at different times, the pressure drop change due to the water distribution inside the inlet and outlet manifolds were observed [15].

In this paper, considering for the first time the hydrophilicity of graphite plate (GP) and the hydrophobicity of GDL, which form the walls of the gas channels, using the VOF model of FLUENT software, the motion of liquid water under different gas velocity is simulated in a straight channel and a serpentine channel. In the following, the computation domain, solution procedure and mesh independency are introduced. Then the results from the cases with different initial gas velocity are presented and analyzed. Finally, some interesting conclusions are drawn.

## 2. Numerical model, methodology and boundary conditions

### 2.1. Computation domain

The typical cathode gas channels of PEMFC are straight or serpentine, two kinds of such channels are chosen as shown in Fig. 1(a) and (b). The length of the straight channel and the serpentine channel is 11.5 and 23 mm, respectively; both channels' cross-sectional area is 1 mm × 1 mm.

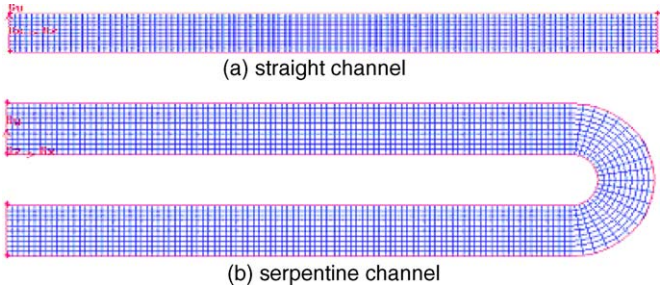


Fig. 1. Geometries of cathode channels.

### 2.2. Computational methodology

The numerical simulation for a 3D transient two-phase flow in the straight and serpentine channels are carried out using VOF model in FLUEN 6.1.22 software, which is suitable to trace the position of the interface between fluids. The flow in the channels is supposed as laminar, as the Reynolds numbers under different velocity in the cases of this paper is no more than 600. Meanwhile the flow is also considered as isothermal and without phase change. Therefore the VOF model transportation equations are as the following [16]:

$$\frac{\partial \alpha_q}{\partial t} + \vec{u} \cdot \nabla \alpha_q = \frac{S_{\alpha_q}}{\rho_q} \tag{1}$$

$$\frac{\partial}{\partial t}(\rho \vec{u}) + \nabla \cdot (\rho \vec{u} \vec{u}) = -\nabla p + \nabla \cdot [\mu(\nabla \vec{u} + \nabla \vec{u}^T)] + \rho \vec{g} + \vec{F} \tag{2}$$

$$\sum_q^n \alpha_q = 1 \tag{3}$$

$$\rho = \sum \alpha_q \rho_q \tag{4}$$

For the flow in the channels considered, there are only two phases of air and liquid water, the source item in momentum Eq. (2) caused by surface tension and wall surface adhesion is

$$\vec{F} = \frac{2\sigma_{ij}\rho k_i \nabla \alpha_i}{\rho_i + \rho_j} \tag{5}$$

### 2.3. Boundary conditions

A no-slip boundary condition is applied to the gas channel walls. A velocity inlet boundary condition is applied at the air inlet of the inlet flow manifold. At the outlet, the boundary condition is assigned as pressure outlet. Temperature is supposed as 70 °C, at which the real fuel cell operates often. Some parameters, such as surface tension, are chosen according to this temperature.

### 2.4. Validation of grid independent

There are 11,500 and 22,000 cells meshed in two computation domains, and a water droplet of 0.2 mm radius is separated into 32 cells. Grid independency is tested by increasing and decreasing the number of grid cells by 20% for the straight channel, the

flow phenomena in the channel is almost the same, hence the computation results are considered grid independent.

### 2.5. Effects of inertia force, surface tension and viscous force on the flow

To simulate liquid water behavior under various gas velocities, the hydrophilicity of GP and hydrophobicity of GDL, the effects of inertia force, surface tension and viscous force on the flow is analyzed next.

In micro-flow channel the effect of surface tension and wall surface adhesion on the flow is very important, the judgment criterion is as following [16,17]:

$$\text{Reynold number } Re_g = \frac{ud}{v_g}, \qquad Re_l = \frac{ud}{v_l}$$

$$\text{Capillary number } Ca = \frac{\mu_l u}{\sigma}$$

$$\text{Weber number } We = \frac{\sigma}{\rho_g u^2 d}$$

As in VOF model velocity in the flow channels is shared by both phases, liquid and gas have the same velocity on their interface. The volume fraction of gas is much larger than that of liquid, therefore gas Reynolds number is used to describe the flow state in the channels. Table 2 shows the initial criterion numbers, it can be seen that the gas Reynolds number under different velocity is no more than 600, hence the flow is laminar. Meanwhile the liquid Reynolds number is used to compare the influence of inertia force and liquid viscous force to the liquid flow. Capillary number is a comparison of liquid viscous force and the surface tension, which can be used to judge which of the two is the main factor affecting the liquid flow; Weber number is a comparison of surface tension and the gas inertia force or the drag force, the former tends to make the liquid droplet stable while the latter tends to deform or break it. When $Re_l \ll 1$, compared with inertia force, viscous force plays the main role in the flow, therefore it is compared further with surface tension, if $Ca \gg 1$, surface tension may be neglected, otherwise surface tension should be considered ($Re_l = 0.1$, $Ca = 10$ for instance, as low Reynolds number flow in pulmonary fibers or micro-porosity medium) [18]. When $Re \gg 1$, compared with viscous force, inertia force plays the main role in the flow, therefore it is compared further with surface tension, if $We \ll 1$ ($We = 1 \times 10^{-3}$, for instance) [19,20], surface tension may be neglected, otherwise it should be considered. The parameter values used to calculate these Numbers are shown in Table 1, and the Number values are shown in Table 2, from which we know that the $Re_l$ number of the flow in the channels is much larger than 1, therefore the *We* number should be considered, under four kind gas velocity conditions surface tension should not be neglected. Additionally, effect of wall adhesion is taken into account by specifying a wall adhesion angle in conjunction with the continuum surface force (CSF) model in the FLUENT throughout the simulation [15].

Table 1
Parameter values

| Parameter | Value |
|---|---|
| Air density (kg m$^{-3}$) | 1.03 |
| Hydraulic diameter (m) | $1 \times 10^{-3}$ |
| Air dynamic viscosity (Pa s) | $2.0425 \times 10^{-5}$ |
| Air kinematic viscosity (m$^2$ s$^{-1}$) | $1.998 \times 10^{-5}$ |
| Water dynamic viscosity (Pa s) | $4.06 \times 10^{-4}$ |
| Water kinematic viscosity (m$^2$ s$^{-1}$) | $4.15 \times 10^{-6}$ |
| Surface tension (N m$^{-1}$) | $7.2 \times 10^{-2}$ |

Table 2
Reynolds number, Capillary number and Weber number

| Parameter | Value | | | |
|---|---|---|---|---|
| Gas velocity (m s$^{-1}$) | 2 | 4 | 6 | 10 |
| $Re_g$ | 100 | 200 | 300 | 500 |
| $Re_l$ | 4819.3 | 9638.6 | 14457.8 | 24096.4 |
| *Ca* | 1.13 | 2.26 | 3.38 | 5.64 |
| *We* | 17.5 | 4.4 | 1.9 | 0.7 |

## 3. Results and discussions

### 3.1. Motion of a single water droplet in straight channel

The contact angle between liquid water and the surface of GDL is 140°, that between liquid water and the wall surface of GP is 70°; the water drop radius is 0.2 mm, at the beginning it is at the center of the channel and on the surface of GDL.

Fig. 2 is the motion state of the droplet on the surface of GDL under different Weber numbers (or different velocities), the color is a scale of the volume fraction of liquid water, the redder it is, the larger the liquid fraction is. For different velocities or Weber numbers different moments are chosen to show the distinct characteristics of the droplet motion in the channels. When velocity is 2 m s$^{-1}$, according to the analysis in Section 2.5, Weber number is 17.5, the influence of surface tension and wall surface adhesion to the motion of the droplet is quite strong, and under low velocity the droplet's deformation is small, the distance between the water droplet and the walls of the GP is long enough so that the hydrophilicity of GP seems have no effect on the droplet's motion. About 5.5 ms late it is discharged as a full but deformed water droplet, as shown in Fig. 2(a). When the gas velocity is 4 m s$^{-1}$, Weber number is 4.4, the inertia force is increased and the deformation is large, the droplet is divided into three, the two child droplets near the two side walls of the GP are gradually attracted onto the walls separately, and the middle child droplet is still on the surface of GDL (Fig. 2(b)). Finally the three smaller droplets are blown out of the channel gradually. As the gas velocity increased to 6 m s$^{-1}$, Weber number is decreased to 1.9, the inertia force is increased further and the deformation is larger, but the velocity is so high that the water droplet is discharged out of the channel before it is broken, see Fig. 2(c). If the channel were longer, the breaking would possibly happen. When the gas velocity is 10 m s$^{-1}$, Weber number is decreased to 0.7, the inertia force is increased so much that it breaks the droplet into two parts, which are blown out almost at the same

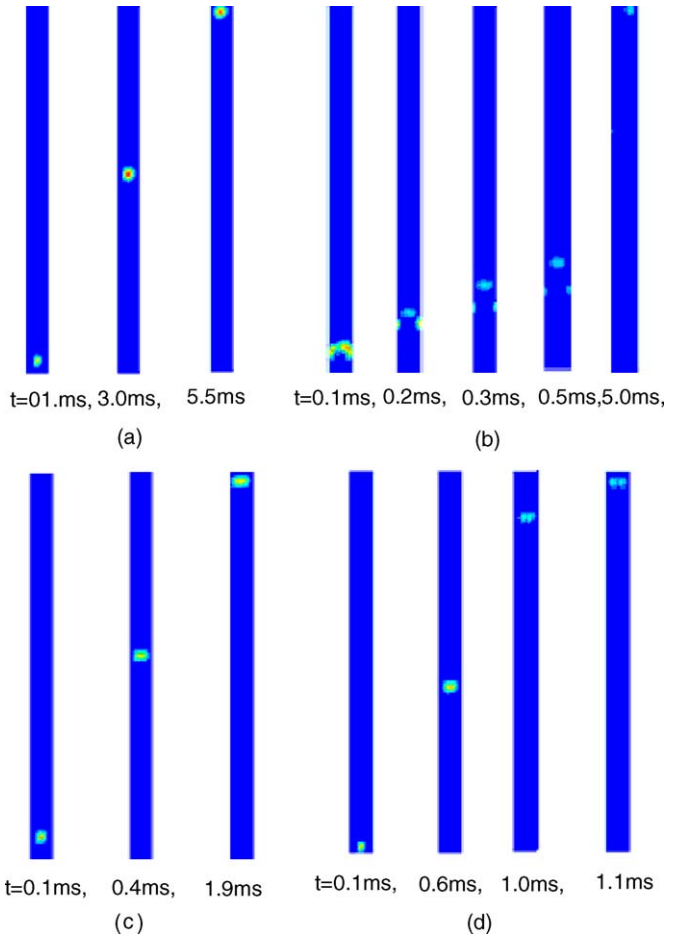


Fig. 2. Water droplet motion in straight channel under different Weber numbers: (a) $We = 17.5$ ($u = 2\,m\,s^{-1}$); (b) $We = 4.4$ ($u = 4\,m\,s^{-1}$); (c) $We = 1.9$ ($u = 6\,m\,s^{-1}$); (d) $We = 0.7$ ($u = 10\,m\,s^{-1}$).

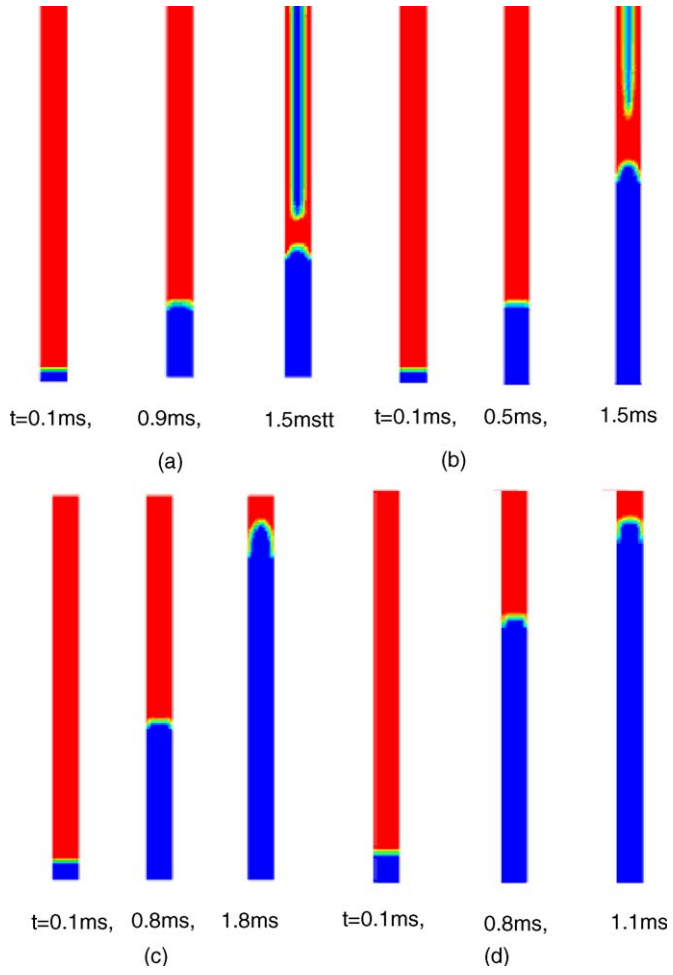


Fig. 3. Water film motion in straight channel under different Weber numbers: (a) $We = 17.5$ ($u = 2\,m\,s^{-1}$); (b) $We = 4.4$ ($u = 4\,m\,s^{-1}$); (c) $We = 1.9$ ($u = 6\,m\,s^{-1}$); (d) $We = 0.7$ ($u = 10\,m\,s^{-1}$).

time, as shown in Fig. 2(d). The time lapsed when the water droplet is blown out of the channel under four different Weber numbers is 5.5, 5.0, 2.0, and 1.2 ms.

### 3.2. Motion of water film in straight channel

When at large current density much water may appear in cathode gas channel and very possibly exists there as water film. If so what characteristic its motion has? Suppose the contact angle between liquid water and the surface of GDL is 140°, that between liquid water and the wall surface of GP is 70°, water film thickness is 0.2 mm, at the beginning it covers the whole surface of the GDL in the channel.

Figs. 3 and 4 are the motion states of the water film on the surface of GDL under different Weber numbers (or different velocities) and water flow rate at the outlet of the channel respectively. As the direction of the droplet motion is the same as the normal of the outlet, the flow rate is expressed as negative in FLUENT. For Fig. 4, $x$-coordinate is the time lapsed, $y$-coordinate is the liquid water flow rate. Fig. 5 is the distribution of the water film on the cross-sections normal to flow direction. When $We = 17.5$, the inertia force is weak while the surface tension and the wall surface adhesion is relatively strong, water film on GDL are gradually attracted onto the walls of GP, hence a no-water-zone on GDL in the center of the channel appears, as shown in Figs. 3(a) and 5(a), of course this phenomena is beneficial to the diffusion of oxygen from the gas channel to the catalyst layer. Water flow rate at the outlet is decreased first, then after a sudden increasing happens it decreases to zero, which means no water leaved in the channel, see Fig. 4(a). This is because the water film on GDL are gradually attracted onto the walls of GP, and the gas flow pushes the film forward, but the resistance "piles" the water near the end of the film, as shown in Fig. 5(a). When $We = 4.4$ ($u = 4\,m\,s^{-1}$), the behavior of the film's motion is similar to that of $We = 17.5$, but the inertia force is large, more water has been blown out before the film on the surface of GDL is attracted to the walls of GP, therefore the no-water-zone on GDL in the center of the channel appears later than that of $We = 17.5$, see Figs. 3(b), 4(b) and 5(b). When $We = 1.9$ and $We = 0.7$, the inertia force plays a more important role for the water film's motion, only part of the water on the surface of GDL is attracted to the walls of GP, and there isn't a no-water-zone appears on GDL during the whole process of the water film's moving out, as shown in Figs. 3–5(c and d). For four different Weber numbers (or velocities) the flux rate is increased

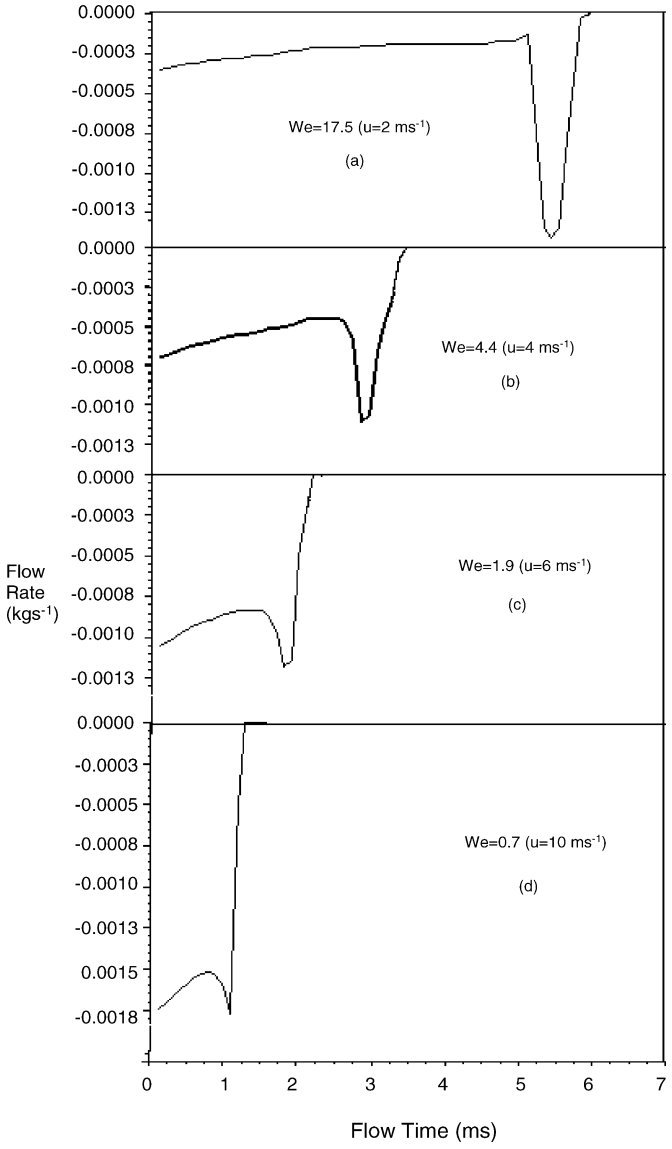


Fig. 4. Flow rate of liquid water film at outlet of straight channel.

gradually, the time for the film to be blown out of the channel is decreased, i.e. 6.0, 3.5, 2.5 and 1.3 ms, respectively.

### 3.3. Motion of a single water droplet in serpentine channel

The contact angle between liquid water and the surface of GDL is 140°, that between liquid water and the wall surface of GP is 70°; the water droplet radius is 0.2 mm, at the beginning it is at the center of the channel and on the surface of GDL. The characteristics of droplet motion in a serpentine channel are more complex than in a straight channel. Fig. 6 is the motion states of the water droplet on the surface of GDL under different velocity. The droplet is a whole one before the turn under all four kind Weber numbers (or velocities), but the deformation is different. This is because, although the inlet velocity and the outlet pressure applied to this serpentine channel are the same as applied to the straight channel, but the length of the former is one time longer than the later, the gas stream is resisted at

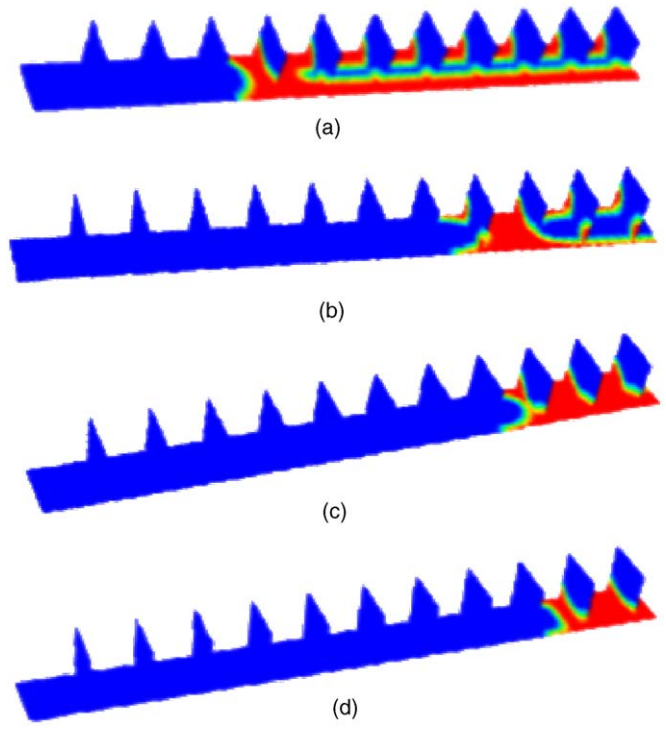


Fig. 5. Water film on the cross-sections normal to flow direction for the film motion in straight channel under different Weber numbers: (a) $We = 17.5$ ($u = 2\,\mathrm{m\,s^{-1}}$), $t = 1.5$ ms; (b) $We = 4.4$ ($u = 4\,\mathrm{m\,s^{-1}}$), $t = 2.0$ ms; (c) $We = 1.9$ ($u = 6\,\mathrm{m\,s^{-1}}$), $t = 1.5$ ms; (d) $We = 0.7$ ($u = 10\,\mathrm{m\,s^{-1}}$), $t = 1.0$ ms.

the turn, therefore water droplet's speed is lower than the corresponding cases of the straight channel, the inertial force and the resistance force applying to the droplet only makes its shape changed, as Fig. 6(a–d) shown. Under higher inlet velocities, the gas stream at the turn changes its flow direction more drastically, the droplet dragged by the stream will change its trace earlier, after a longer distance it will meet the wall of the GP, but the position of the collision is nearer to the outlet of the channel under higher velocity, as shown in Fig. 7, in other word, under a higher gas velocity, the water droplet can be more easily passed the turn and so more easily discharged out of the channel.

Moreover, it can be seen from Fig. 6 that at the turn only when $We = 0.7$ ($u = 10\,\mathrm{m\,s^{-1}}$) the droplet breaking happens, and it meets the wall of the channel. After the turn the droplet under four cases comes onto the upper-external sides of the gas channel wall, as shown in Fig. 8, owing to gas stream eddy and the hydrophilicity of GP. The droplet breaks when $We = 4.4$ ($u = 4\,\mathrm{m\,s^{-1}}$), $We = 1.9$ ($u = 6\,\mathrm{m\,s^{-1}}$) and $We = 0.7$ ($u = 10\,\mathrm{m\,s^{-1}}$). The time for the droplet to be blown out of the channel under four Webers is 90, 28, 16 and 6.5 ms, respectively.

### 3.4. Motion of water film in serpentine channel

Suppose water appears in cathode gas channel as water film under large current density. The contact angle between liquid water and the surface of GDL is 140°, that between liquid water

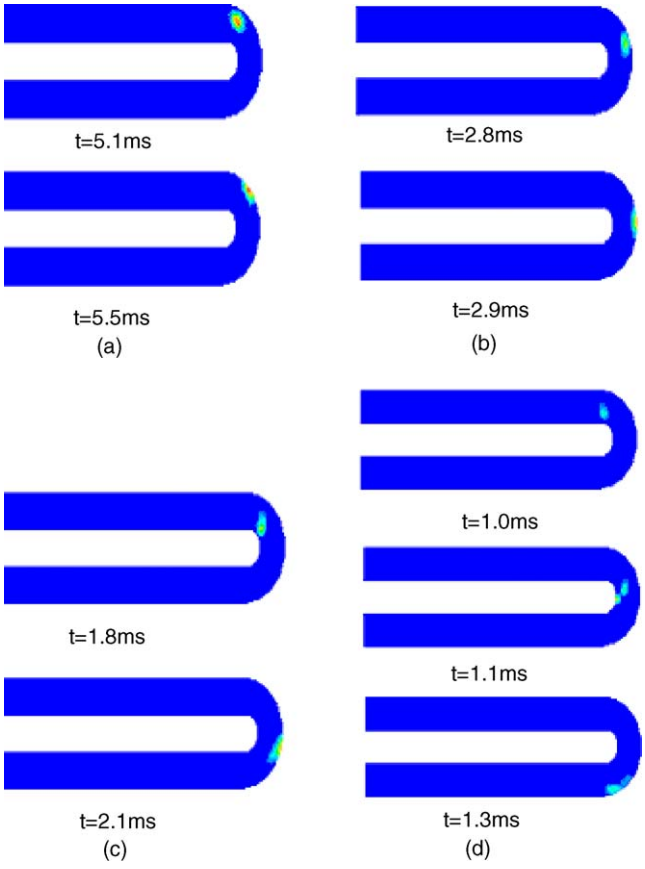


Fig. 6. Water droplet motion at the turn in serpentine channel under different Webers: (a) $We = 17.5$ ($u = 2\,\mathrm{m\,s^{-1}}$); (b) $We = 4.4$ ($u = 4\,\mathrm{m\,s^{-1}}$); (c) $We = 1.9$ ($u = 6\,\mathrm{m\,s^{-1}}$); (d) $We = 0.7$ ($u = 10\,\mathrm{m\,s^{-1}}$).

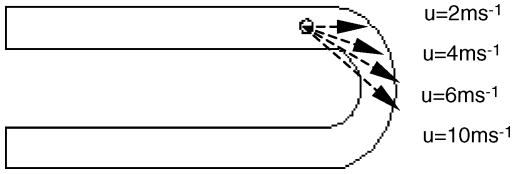


Fig. 7. Traces of the droplet at the turn under different Webers.

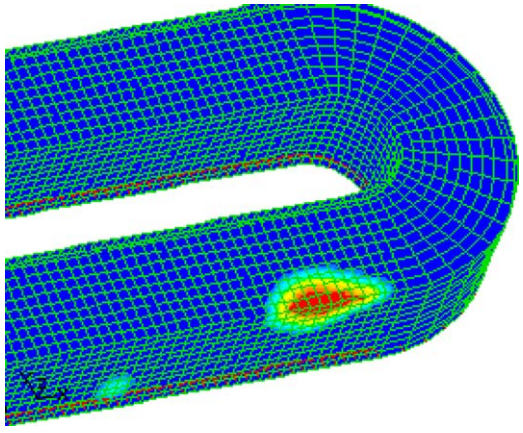

Fig. 8. State of the droplet after the turn.

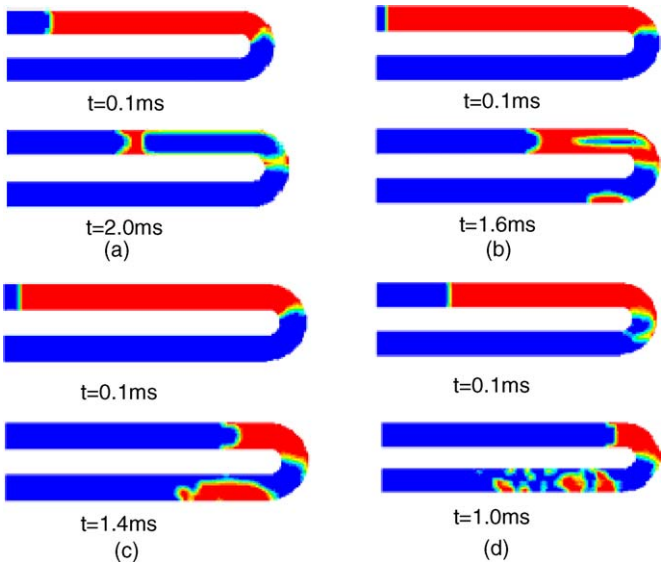


Fig. 9. Water film motion in serpentine channel under different Weber numbers: (a) $We = 17.5$ ($u = 2\,\mathrm{m\,s^{-1}}$); (b) $We = 4.4$ ($u = 4\,\mathrm{m\,s^{-1}}$); (c) $We = 1.9$ ($u = 6\,\mathrm{m\,s^{-1}}$); (d) $We = 0.7$ ($u = 10\,\mathrm{m\,s^{-1}}$).

and the wall surface of GP is 70°, film thickness is 0.2 mm. In order to investigate the behavior of the film at the turn, the water film exists only at the first half of the channel, at the beginning it covered the surface of the GDL in the channel.

Figs. 9 and 10 are the motion states of the water film on the surface of GDL under different Weber numbers. Fig. 11 is the water flow rate at the outlet of the channel. When $We = 17.5$ ($u = 2\,\mathrm{m\,s^{-1}}$), the inertia force is weak while the wall surface adhesion is relatively strong, from Figs. 9(a) and 10(a) it can be seen that under the action of the gas stream the water film is pushed forward, and is attracted on to the walls of the GP, finally a no-water-zone appears, similar to Fig. 3(a). Meanwhile the hydrophilic walls of GP attracted more and more water. After the turn the water film is mainly on the hydrophilic walls and relatively centralized, only a little part on GDL, until discharged out of the channel, see Fig. 11(a). When $We = 4.4$ ($u = 4\,\mathrm{m\,s^{-1}}$), the situation is similar to that of $We = 17.5$ ($u = 2\,\mathrm{m\,s^{-1}}$), but because the velocity is higher, the inertia force is larger, water film moved forward quickly, the phenomena described as above appears later, see Figs. 9(b) and 10(b). Meanwhile at the turn and after the turn the distribution of the water film is more disperse, as Fig. 11(b) shows. When $We = 1.9$ ($u = 6\,\mathrm{m\,s^{-1}}$) and $We = 0.7$ ($u = 10\,\mathrm{m\,s^{-1}}$), because the inertia force plays the main role, although part of the film is attracted onto the hydrophilic walls of GP, as shown in Figs. 9(c) and (d) and 10(c) and (d), but no no-water-zone formed on GDL, which is the same as Fig. 3(c) and (d). At the turn and after the turn the distribution of the water film is further more disperse, see also Fig. 11(c) and (d), the drastic fluctuating of the water flow rate curves demonstrates such a behavior. Because the gas velocity is different, the time spent for the same quality of liquid water to be blown out has difference, i.e. 26, 17, 9.0 and 4.5 ms, respectively.

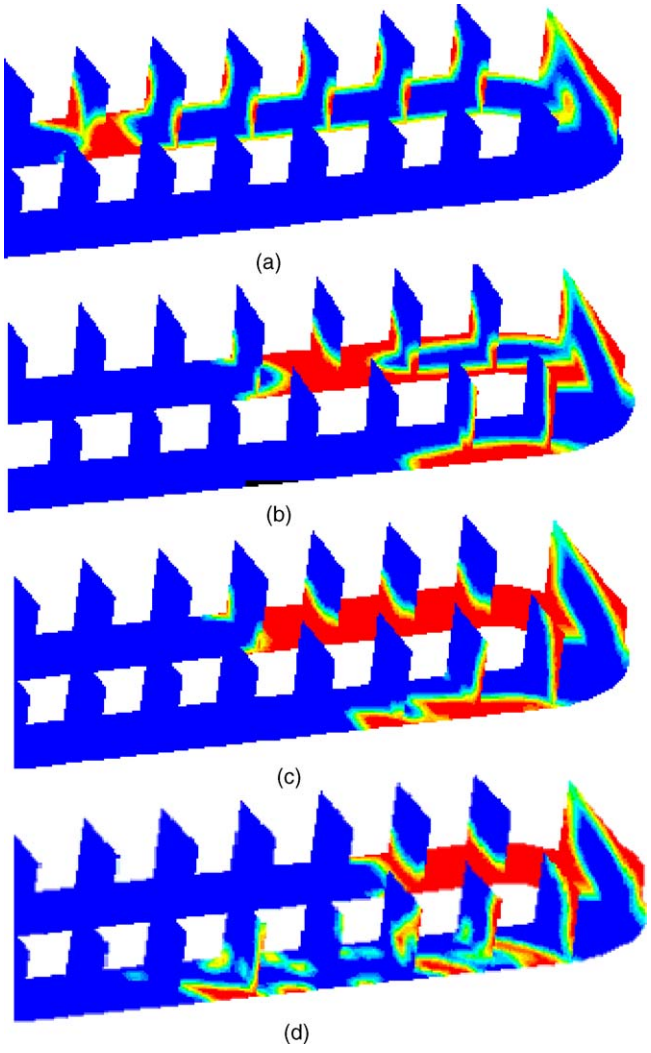


Fig. 10. Water film on the cross-sections normal to flow direction for the film motion in serpentine channel under different Weber numbers: (a) $We = 17.5$ ($u = 2\,\mathrm{m\,s^{-1}}$), $t = 2.0\,\mathrm{ms}$; (b) $We = 4.4$ ($u = 4\,\mathrm{m\,s^{-1}}$), $t = 1.6\,\mathrm{ms}$; (c) $We = 1.9$ ($u = 6\,\mathrm{m\,s^{-1}}$), $t = 1.0\,\mathrm{ms}$; (d) $We = 0.7$ ($u = 10\,\mathrm{m\,s^{-1}}$), $t = 1.0\,\mathrm{ms}$.

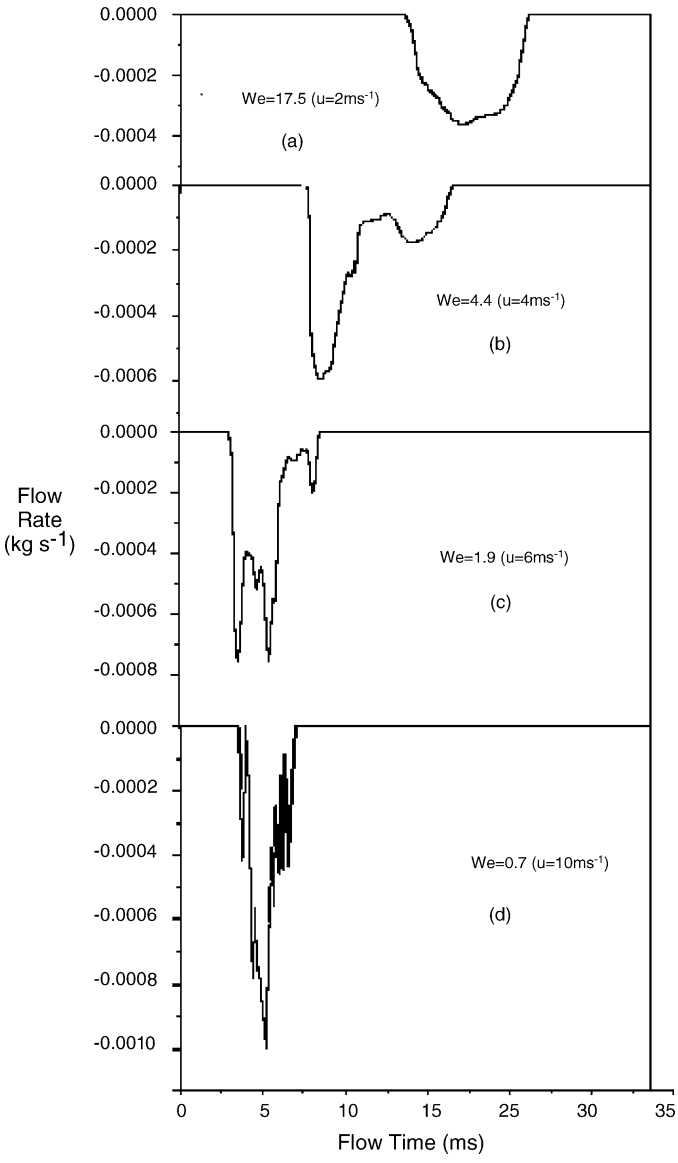


Fig. 11. Flow rate of liquid water film at outlet of serpentine channel.

### 3.5. *Effect of surface treatment to the flow*

From previous analysis we can see that the hydrophilicity of GP and the hydrophobicity of the GDL play an important role in the motion of liquid water in the gas channel. In order to explore the effect to the flow of different hydrophilicity of GP and hydrophobicity of the GDL, two sets of cases are simulated, under each case the whole surface of the GDL in straight channel is covered initially by 0.2 mm thick water film, the gas velocity is $2\,\mathrm{m\,s^{-1}}$, $We = 17.5$; under Set 1 the contact angle between liquid water and the surface of GDL is fixed as 140°, that between liquid water and the wall surface of GP is as 0°, 45°, 70°, 90°, 140° and 180°; under Set 2 the contact angle between liquid water and the surface of GP is fixed as 70°, that between liquid water and the surface of GDL is as 0°, 45°, 70°, 90°, 140° and 180°. Fig. 12 shows the result, on which $y$-coordinate is the time lapsed before the whole water film is discharged out of the channel, $x$-coordinate is the contact angle between liquid water and the wall surface of GP for Set 1, or the contact angle

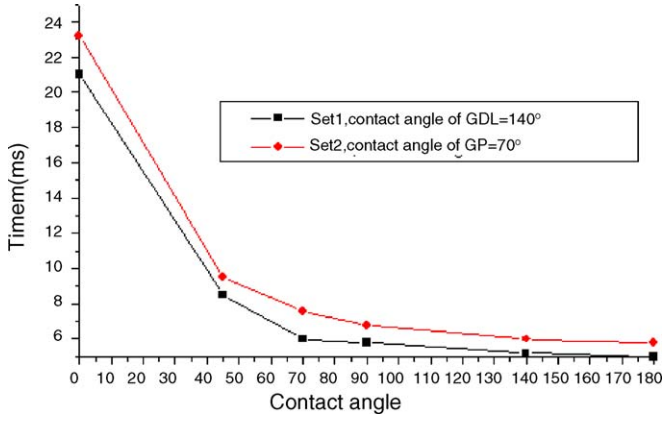


Fig. 12. Time used to discharge the water film vs. contact angle under $We = 17.5$ ($u = 2\,\mathrm{m\,s^{-1}}$).

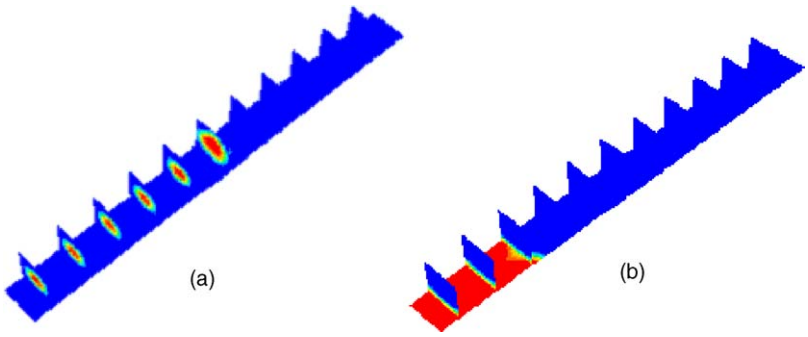


Fig. 13. Distribution of the water film for different contact angles, $We = 17.5$ ($u = 2\,m\,s^{-1}$): (a) contact angles for GDL and GP are 140° and 180°, respectively, $t = 2.4$ ms; (b) contact angles for GDL and GP are 0° and 70°, respectively, $t = 22$ ms.

between liquid water and the surface of GDL for Set 2. It' can be seen that the time used to discharge the water decreases with the increasing of the contact angle between liquid water and the wall surface of GP for Set 1, and with the increasing of the contact angle between liquid water and the surface of GDL for Set 2. For Set 1, the maximum time is 21 ms when the contact angle between liquid water and the surface of GP was 0°, which is about four-fold the time when the contact angle between liquid water and the surface of GP was 180°. For Set 2 a similar result can be gotten. That is to say, the more hydrophobic the surfaces of the channel are, the more easily the water is to be discharged.

Meanwhile the distribution of the water film in the channel should be considered. Fig. 13 is the distribution of the water film of two cases with different contact angles. Fig. 13(a) is the water distribution of a case at $t = 2.4$ ms, under which the contact angles of GDL and GP are 140° and 180°, respectively. Although under such a case the time used to discharge the water is the least, only 5.0 ms, but the water film changes into a water column, which blocks the gas flow and impedes the diffusion of oxygen from the channel to catalyst layer. Fig. 13(b) is the water distribution of another case at $t = 8.2$ ms, where the contact angles of GDL and GP are 0° and 70°, respectively. The time used to discharge the water is 23.2 ms, at all time the water film covers at least part of the surface of GDL, which impedes severely the diffusion of oxygen form the channel to catalyst layer. Another typical case is as Fig. 5(a) shown, where the contact angles of GDL and GP are 140° and 70°, respectively. Under such a case the time used to discharge the water is 6.0 ms, but water film on GDL are gradually attracted onto the walls of GP, hence a no-water-zone on GDL in the center of the channel appears, which is beneficial to the diffusion of oxygen from the gas channel to catalyst layer.

In summary, in order to enable the liquid water to be discharged easily out of the gas channel, and to make oxygen to diffuse from the gas channel to catalyst layer conveniently, GDL should be as hydrophobic as possible while GP should be suitably hydrophilic.

## 4. Conclusions

The hydrophilicity of GP and the hydrophobicity of the GDL play an important role in the motion of liquid water in the gas channel.

The more hydrophobic the surfaces of the channel are, the more easily the water is to be discharged. The hydrophilicity of GP can attract the liquid water from GDL onto the walls of the GP, which is beneficial to the diffusion of oxygen from the gas channel to the catalyst layer. Therefore GDL should be as hydrophobic as possible while GP should be suitably hydrophilic.

Of the computed cases, when Weber number is larger than 4.4 (gas velocity is lower than $4\,m\,s^{-1}$), effects of surface tension and wall surface adhesion on the motion of liquid water in the gas channel are very obvious; when Weber number is less than 4.4 (gas velocity is higher than $4\,m\,s^{-1}$), inertia force plays the main role in the motion of liquid water in the gas channel.

Liquid water is more easily discharged out of the channel under high gas velocity than under lower velocity; compared with serpentine channel, liquid water in straight channel is more easily discharged.

As the length of the channel chosen is short, only to some extent do the results in this paper reveal the motion characteristics of the water droplet and water film in the gas channel, the gas diffusion, the production of the liquid water and its transportation in fuel cell have been coupled neither. The relative research needs to be continued.

## Acknowledgments

The authors acknowledge the financial support of the Natural Science Foundation of Hubei, China (2003ABA088) and the Special Scientific Research Foundation for College Doctor Subjects from Ministry of Education of China (No. 20030497012).

## References

[1] F. Meier, G. Eigenberger, Electrochim. Acta 49 (2004) 1731–1742.
[2] G. Karimi, X. Li, J. Power Sources 140 (2005) 1–11.
[3] H.M. Yu, C. Ziegler, M. Oszcipok, M. Zobel, C. Hebling, Electrochim. Acta 51 (2005) 1199–1207.
[4] C.S. Kong, D.Y. Kim, H.K. Lee, Y.G. Shul, T.H. Lee, J. Power Sources 108 (2002) 185–191.
[5] J.H. Nam, M. Kaviany, Int. J. Heat Mass Transf. 46 (2003) 4595–4611.
[6] A.B. Geiger, A. Tsukada, E. Lehmann, P. Vontobel, A. Wokaun, G.G. Scherer, Fuel Cell 2 (2002) 92–98.
[7] R. Satija, D.L. Jacobson, M. Arif, S.A. Werner, J. Power Sources 129 (2004) 238–245.

[8] K. Tuber, D. Pocza, C. Hebling, J. Power Sources 124 (2003) 403–414.
[9] X.G. Yang, F.Y. Zhang, A.L. Lubawy, C.Y. Wang, Electrochem. Solid-State Lett. 7 (11) (2004) A408–A411.
[10] S. Dutta, S. Shimpalee, J.W. Van Zee, Int. J. Heat Mass Transf. 44 (2001) 2029–2042.
[11] T. Berning. PhD Dissertation of the University of Victoria, Canada, 2002.
[12] X. Li, U. Becker, Second International Conference on Fuel Cell Science, Engineering and Technology Rochester, NY, 2004.
[13] S. Um, C.Y. Wang, J. Power Sources 125 (2004) 40–51.
[14] Q. Peng, Z. Biao, A. Sobiesiaka, Z.S. Liu, J. Power Sources 152 (2005) 131–145.
[15] K. Jiao, Z. Biao, Q. Peng, J. Power Sources, in press.
[16] FLUENT 6. 0 Users Guide Documentation, FLUENT Inc., Lebanon, New Hampshire, 2001.
[17] B. Cai, L. LI, Z.L. Wang, J. Eng. Thermophys. 24 (4) (2003) 613–616.
[18] S.X. Xu, Y.T. Chen, H.T. Low, L. Ji, L. Lu, J. Hydrodynam. 16 (1) (2001) 35–43.
[19] P. Wang, S.Z. Wang, Ship Sci. Technol. 27 (2) (2005) 77–80.
[20] X.S. Shao, D.G. Xi, J.R. Qin, G.C. Shu, N. Liu, J. Combust. Sci. Technol. 2 (4) (1996) 307–314.